CDF/ANAL/JET/PUBLIC/5507
December 21, 2000

Frascati Physics Series Vol. nnn (2001), pp. 000-000

IX INT. CONF. ON CALORIMETRY IN PART. PHYS. - Annecy, Oct. 9-14, 2000

STUDIES OF JET ENERGY RESOLUTIONS. Lami^a, A. Bocci^a, S. Kuhlmann^b, G. Latino^c*a) The Rockefeller University, New York, NY 10021, USA**b) Argonne National Laboratory, Argonne, IL 60439, USA**c) University of Cassino and INFN Pisa, Italy*

presented by Stefano Lami, on behalf of the CDF Collaboration

ABSTRACT

The jet energy resolution comes from many sources, which can be grouped into two categories, detector and physics effects. We studied the physics uncertainties using simulated $W \rightarrow jj$ events in order to improve the low-mass tail in the di-jet mass distribution. For the detector resolution we used both CDF detector simulation and data. For the first time the full granularity of the CDF detector is used to perform corrections at “tower level” rather than at “jet level”. The track momenta measured by the Central Tracking Chamber (CTC) and the neutral cluster energies measured by the Central Shower Max (CES) are used to correct the calorimeter tower energies. When tested on $\gamma + jet$ data, our new algorithm has shown an improvement on the jet energy resolution better than 20% compared to the standard CDF jet corrections.

1 Introduction

Run II at the Tevatron Collider will start in spring 2001 and the upgraded CDF experiment will have greatly improved sensitivity in the search for the Higgs bosons of the Standard Model and minimal Supersymmetry. The study of the di-jet mass resolution for Run II is very important as many new physics

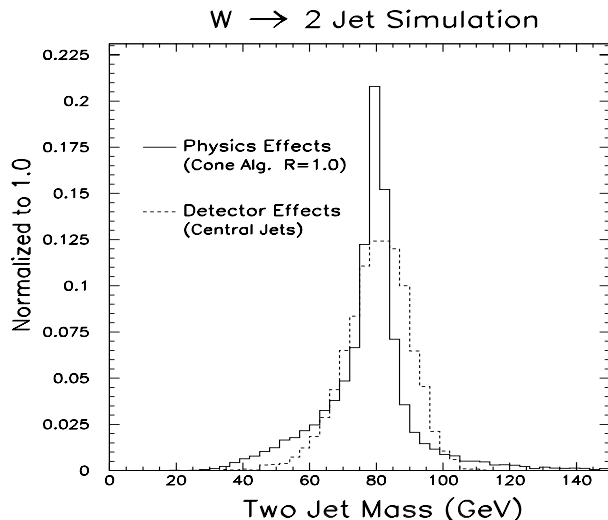


Figure 1: *The $W \rightarrow q\bar{q}$ mass distribution with pure algorithm effects (solid), and pure detector effects (dashed).*

signatures are expected to appear as multi-jet mass bumps. In the case of the neutral Higgs boson, it dominantly decays into $b\bar{b}$ for a mass within the Tevatron reach, and the improvement of the di-jet mass resolution in the CDF detector is crucial.

A couple of years ago we started a very general study on jet algorithms for the CDF detector. The jet energy resolution comes from many sources, but they can be grouped into two categories: (1) detector effects such as calorimeter resolution, and (2) physics effects such as fluctuations in the energy outside a clustering cone. The purpose of our study is to consider separately jet reconstruction uncertainties coming from “physics” which would be present also if the energy of each particle in the jet would be exactly known, and uncertainties due to the detector resolution. Fig. 1 shows the di-jet mass distribution from a $W \rightarrow q\bar{q}$ simulation. The solid histogram is the particle level mass distribution using a cone algorithm with a radius 1.0, without including detector effects. The dashed histogram is the mass distribution with only CDF detector effects, with the algorithm effects removed by using the known particle list. One can see that the two distributions are quite different, with the detector

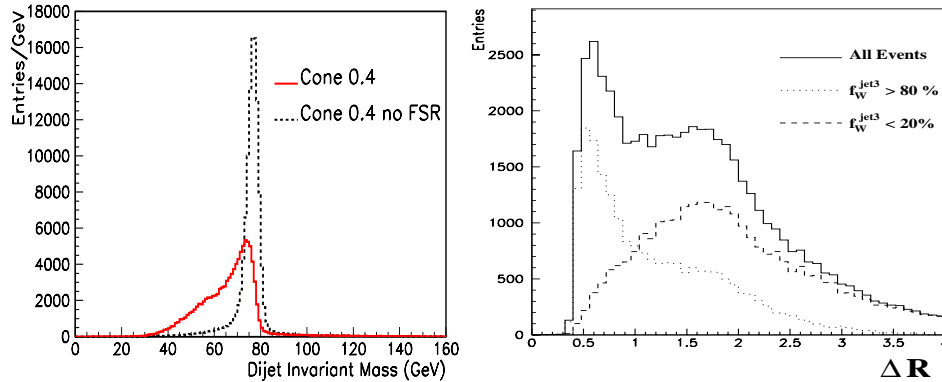


Figure 2: *Left: the di-jet invariant mass for cone 0.4 is shown with FSR turned on (solid curve) and off (dashed). Right: the ΔR separation between the third jet and the closest leading jet, for all events (solid) and the two cases of a large (dotted) and small (dashed) W energy fraction.*

effects tending to dominate the central core of the distribution, $\sigma = 9$ GeV compared to $\sigma = 4$ GeV, while the algorithm effects dominating the tails.

2 Physics Effects

We considered four different physics effects that contribute to the W di-jet mass resolution: 1) the natural width of the decaying object; 2) the underlying event fluctuations, which give a gaussian contribution with a width ~ 2 GeV and therefore were not further investigated, as the nominal gaussian width from detector effects is much larger than this; 3) misidentified leading jets from initial state gluon radiation (ISR), which mainly contribute to the high mass tail, and can be reduced by either increasing the jet P_T cutoff, or decreasing the jet η limits; 4) the final state gluon radiation (FSR), which causes a significant tail at low masses, as shown in fig. 2(left) for a cone of radius 0.4, is the dominant effect and is also the effect which is universal to all analyses. In order to improve the low mass tail of the W mass distribution, we first investigated different jet algorithms like for instance the K_T algorithm, but we found it equivalent to the cone algorithm, for the same cluster dimension, at least for this physics with two isolated light quark jets. We then returned to the cone algorithm with a cone radius of 0.4 and studied the merging of extra jets and forming

the multijet mass. The energy cutoff for merging was determined to reduce jets from ISR. Fig. 2(right) shows the ΔR separation between the two leading jets and the third jet. We defined two classes of events based on the third jet W energy fraction, those with W energy fraction greater than 80% (dotted), and those with W energy fraction less than 20% (dashed). The solid histogram is the ΔR separation for all events. A merging radius of 1.0 is optimal. We also performed a likelihood analysis under the hypothesis of background and signal+background, and the best improvement was found for a cone 1.0 and a cut on the third jet $P_T < 8$ GeV, that we will use in the following.

3 Detector Effects

The standard CDF jet algorithm uses the calorimeter information only, and then apply corrections to take into account calorimeter non-linearity, detector cracks, and jet shower leakage. We studied a new method to form the energy of a calorimeter tower including also information from other CDF detector components. For the first time the track momentum by the CTC is used to reduce the non-linearity effect in the measurement performed by the calorimeter. Furthermore, the information from the CES is used to sort out the overlapping particles like π^0 with π^\pm .

3.1 The classification method ¹⁾

The calorimeter towers are divided into four classes, depending on which kind of particles hit the tower, and for each class a different method to determine the energy collected in the tower is adopted. The four tower classes are:

- **Track Tower :** Extrapolating the CTC track to the central calorimeter, we associate track to tower. The towers hit by a track are flagged *Track Tower*. In order to take into account leakage, the adjacent towers in η are considered *Track Tower* as well. The energy associated to the target tower is the sum of the transverse momenta over all charged particles hitting the tower. To avoid double counting, *no energy* is associated to leakage towers.
- **Gamma Tower :** The presence of a photon is provided by energetic clusters in the CES. Leakage towers are also present if the photon falls

Table 1: Tower “classification” for the run 1B photon + jet data sample.

Tower Type	Fraction of towers	Fraction of energy
Track	58.6 %	31.0 %
Gamma	8.8 %	7.9 %
Mixed	17.8 %	57.8 %
N. A.	14.8 %	3.4 %

near the tower edge. The energy associated to these kind of towers is the energy collected by the electromagnetic calorimeter (CEM).

- **Mixed Tower :** When a tower satisfies *both* prescriptions required for “track” and “gamma” towers, it is then labeled as *Mixed*. The energy associated to these tower is a combination of track transverse momenta and CEM energy. To avoid a double counting we subtract an estimate of the charged particle contribution to the CEM energy.
- **Not Assigned Tower :** When a tower satisfies *neither* prescription for “track” and “gamma” tower, it is labeled *Not Assigned*. In our Monte Carlo studies we found that these towers are usually hit by either low energy photons, or neutral hadrons. The calorimetric energy is then assigned to these towers.

As an example, tab. 1 summarizes the “classification” on the photon + jet data sample. There are $\sim 60\%$ of *Track* towers, but they carry $\sim 30\%$ of the event energy. This is due to both shower leakage outside the target tower and high fraction of total energy in *Mixed* towers because of the overlap of energetic particles in the core of the jet. Few towers are *Not Assigned* but they carry a small amount of energy.

3.2 New corrections vs. standard corrections

In order to compare our new jet energy reconstruction with the standard CDF method ²⁾, we used real data to be unquestionably sensitive to detector effects that could be partially unknown or incorrectly reproduced in the simulation. Direct photon data are the ideal sample to compare different jet energy reconstructions in the photon-jet P_T balancing. We used the standard CDF photon selection for run 1B ³⁾ and required a central jet. Furthermore, to extract

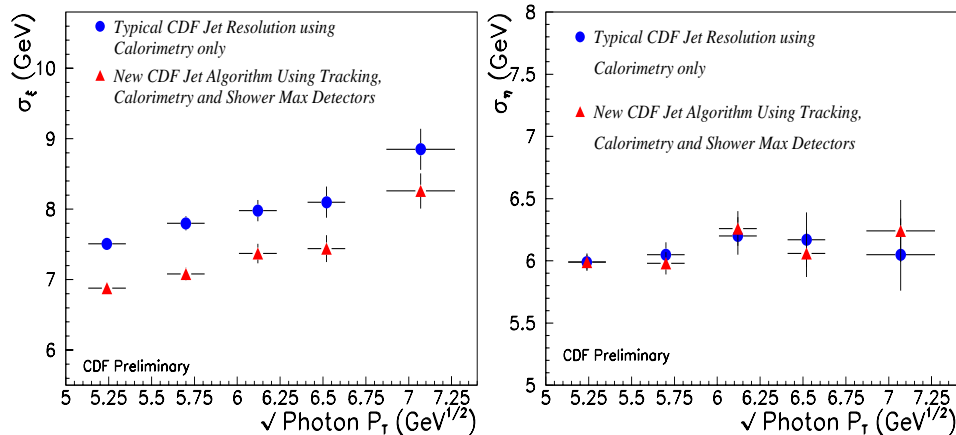


Figure 3: The value of σ_ξ (left) and σ_η (right) are plotted as a function of $\sqrt{P_T^\gamma}$ for the two methods.

a central detector resolution from these data reducing the sensitivity to the physics effects, we adopted a technique à la UA2 where we project the imbalance vector $\vec{P}_T = \vec{P}_T^{jet} + \vec{P}_T^\gamma$ along the azimuthal angular bisectors of the photon-jet system⁴⁾. The two resulting components P_{T_ξ} and P_{T_η} are sensitive to different effects. The calorimeter energy resolution is the main source of the P_{T_ξ} component, while gluon radiation effects are common to both components. So we expect that the width of P_{T_ξ} , σ_ξ , increase with P_T^γ , if it is sensitive to the detector resolution. This is the case, as shown in fig. 3(left), and a significant improvement has been obtained by using the new energy reconstruction (triangles) relative to the standard one (circles). The σ_η width is supposed to have a flat dependence on P_T^γ , and the classification method is not expected to improve this component, as it cannot recover the angular resolution due to physics effects, as shown in fig. 3(right). After hard gluon emission is reduced by applying a cut on the second jet energy, the soft contribution can be removed by subtracting in quadrature σ_η from σ_ξ . In this way we subtract the contribution due to finite angle resolution (σ_η) from the jet energy resolution σ_ξ , and we can define an “effective” detector resolution σ_D for central jets $\sigma_D = \sqrt{\sigma_\xi^2 - \sigma_\eta^2}$. By dividing σ_D by the central value of each P_T^γ bin we obtain the energy resolution plotted in fig. 4 as a function of P_T^γ . There is a significant improvement going from $\sigma/P_T \approx 83\% / \sqrt{P_T}$ using the standard

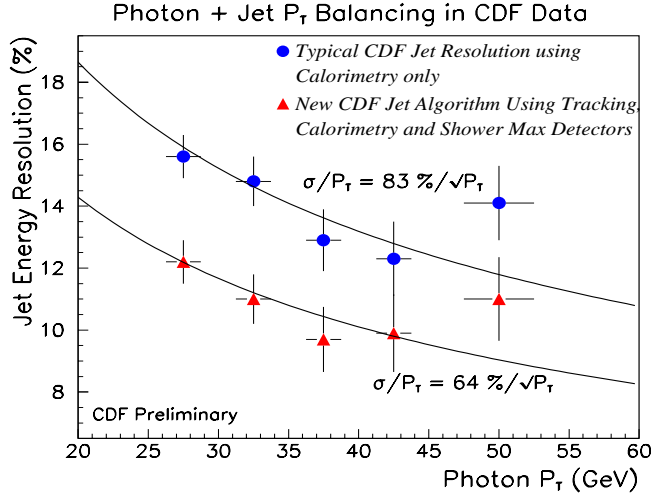


Figure 4: The central detector resolution σ_D is plotted as a function of P_T^γ for the two methods.

CDF corrections, to $\sigma/P_T \approx 64\% / \sqrt{P_T}$ obtained with the new combination of tracking, calorimeter and shower max information.

4 Conclusions

After an exhaustive study of the physics effects that enter in the jet energy resolution, we studied the detector effects and developed a new method to correct for low energy non-linearities of the central calorimeter response. Track momenta and Shower Max clusters have been used to divide the calorimeter towers into different classes and define the tower energy according to the kind of particles hitting the tower. When tested on a $\gamma - jet$ data sample, our “classification method” has shown an improvement on the jet energy resolution better than 20% compared to the standard CDF jet corrections.

References

1. A. Bocci, Laurea thesis, University of Pisa (1998).
2. F. Abe *et al.*, *Phys. Rev. D* **47** 4857 (1993).
3. F. Abe *et al.*, *Phys. Rev. D* **48** 2998 (1993).
4. UA2 collaboration, *Phys. Lett. B* **154** 338 (1985).